

Supporting Information

Gadelha et al. 10.1073/pnas.0909289106

SI Methods

Cell Culture. Bloodstream-form *T. brucei* Lister 427 was maintained in HMI-9 medium (1) supplemented with 15% FCS at 37 °C and 5% CO₂. All procedures below were performed on cell cultures grown to a density of 1 × 10⁶ cells per mL.

Cold Uptake Experiments. To maintain cells at constantly low temperature, all reagents and plasticware were prechilled to 0 °C, whereas centrifuge and rotor were precooled to 4 °C.

Cells were harvested by centrifugation at 800 × *g* for 5 min at 4 °C and resuspended at 2 × 10⁸ cells per mL in PBS plus 20 mM glucose (pH 7.5). They were then held on ice for 10 min before being pulsed with 5-nm colloidal gold (final concentration of 5 × 10¹² particles per mL) conjugated to either BSA (British Biocell International), WGA (EY Labs), or TL (EY Labs). WGA and TL are small lectins that bind to poly-*N*-acetylglucosamine/lactosamine moieties (2–4). As a control for protein-binding specificity, and size exclusion, cells were pulsed with unconjugated colloidal gold (5 × 10¹² particles per mL; British Biocell International) of 5, 10, 15, 20, and 40 nm in diameter. The pulse duration was 15 min on ice, during which time cells remained actively motile and morphologically normal (as assessed by light microscopy). At the end of this period, isothermal glutaraldehyde was added to the system to a final concentration of 2.5%. Fixation was carried out for 10 min on ice, followed by an additional 30 min at room temperature.

To ascertain the number of colloidal gold particles per unit volume, each colloidal gold reagent (conjugated or unconjugated) was serially diluted in water, and a known volume of solution was spread over the surface of Formvar- (Agar Scientific) and carbon-coated, glow-discharged grids. Electron micrographs were taken of five randomly selected areas, and the density of gold particles was estimated by particle counting by using the publicly available ImageJ software (National Institutes of Health).

Fast, Isothermal Aldehyde Fixation. To capture vesicular traffic in an unperturbed state, cells were rapidly fixed in culture by the addition of isothermal glutaraldehyde to the culture flask, making a final concentration of 2.5% while the flask was still in the 37 °C incubator. The culture flask was gently rocked for 10 min, still at 37 °C, after which fixed cells in medium were harvested by centrifugation at 800 × *g* for 5 min and resuspended in 2.5% glutaraldehyde in PBS for another 30 min at room temperature.

High-Pressure Freezing and Freeze Substitution. Cells grown in culture medium supplemented with 2.5% gum arabic (Sigma) were harvested by centrifugation at 800 × *g* for 5 min, transferred to flat gold specimen carriers of 200-μm depth, sealed, and high-pressure-frozen in an EM PACT2 (Leica Microsystems) in ≈10 ms. Specimen carriers were transferred under liquid nitrogen to cryovials containing precooled fixation solution (1% glutaraldehyde/0.1% uranyl acetate in acetone) and were freeze-substituted for 16 h at –90 °C. The fixation solution was replaced with 1% osmium

tetroxide/0.1% uranyl acetate in acetone and freeze-substituted for a further 16 h at –60 °C, after which samples were raised to 0 °C by linear temperature ramping at 10 °C per h. Samples were removed from specimen carriers, washed three times in cold acetone, infiltrated with propylene oxide, and embedded in epoxy resin.

Routine Thin-Section TEM. Fixed cells were postfixed in 1% osmium tetroxide in PBS for 30 min at room temperature, washed five times in double-distilled water, and then en bloc-stained with 1% aqueous uranyl acetate for 2 h at room temperature. Samples were dehydrated through acetone, followed by replacement with propylene oxide, and finally were embedded in epoxy resin. Thin sections (70 nm) were poststained with 2% aqueous uranyl acetate and Reynold's lead citrate.

Thick-Section Electron Tomography. Ribbons of serial thick (250-nm) sections were collected on Formvar-coated copper-rhodium slot grids and poststained with aqueous uranyl acetate and Reynold's lead citrate as above. Colloidal gold particles (15 nm) were deposited on both surfaces of the sections for use as fiducial markers for alignment of the tilted views necessary for tomography. Sections were viewed in an FEI Tecnai-F30 electron microscope operating at 300 keV, and images were captured digitally with a 2k × 2k CCD camera (Gatan) at a magnification that gave 1 nm per pixel. Tilt series were recorded at 1° angular increments over a range of 120° (±60°) about two orthogonal axes with automated microscope control using the SerialEM software (5). The 3D density distributions (tomograms) were calculated by back-projection of each aligned tilt series, and the data from orthogonal series were combined to produce single dual-axis 3D reconstructions measuring 2 × 2 × 0.3 μm³. Reconstructions from adjacent sections were aligned to each other, and subcellular structures and membranes within the 3D volumes were analyzed and modeled. All alignment, reconstruction, montaging, modeling, and analysis were performed by using the IMOD software package (6) version 3.13.5.

Freeze Fracture. Fixed cells were infiltrated with 30% glycerol in PBS for 20 min, frozen by rapid plunging into nitrogen slush, and then freeze-fractured in a BAF 400-T freeze-fracture unit (Balzers) at –115 °C and a vacuum of >10^{–6} mbar. Fractured samples were replicated by electron beam evaporation of platinum–carbon and carbon at angles of 45° and 90°, respectively. Replicas were cleaned with hypochlorite solution, rinsed in distilled water, and mounted onto grids.

Online Movies. The images presented in Figs. 2 and 3 are selected slices extracted from a tomographic reconstruction and model. **Movie S1** shows a complete 3D tomographic reconstruction; **Movie S2** shows the same reconstruction merged with the resultant 3D model; and **Movie S3** shows the 3D model rotated by 360° around the *x* axis. QuickTimePro version 7.5 (Apple) was used to generate all three movies from IMOD-exported Tiffs, using H.264 compression. Movie frame rates are 10 frames per s.

1. Hirumi H, Hirumi K (1989) Continuous cultivation of *Trypanosoma brucei* bloodstream forms in a medium containing a low concentration of serum-protein without feeder cell layers. *J Parasitol* 75:985–989.
2. Atrih A, Richardson JM, Prescott AR, Ferguson MAJ (2005) *Trypanosoma brucei* glycoproteins contain novel giant poly-*N*-acetylglucosamine carbohydrate chains. *J Biol Chem* 280:865–871.
3. Brickman MJ, Balber AE (1990) *Trypanosoma brucei rhodesiense* bloodstream forms: Surface ricin-binding glycoprotein are localized exclusively in the flagellar pocket and the flagellar adhesion zone. *J Protozool* 37:219–224.

4. Nolan DP, Geuskens M, Pays E (1999) N-linked glycans containing linear poly-*N*-acetylglucosamine as sorting signals in endocytosis in *Trypanosoma brucei*. *Curr Biol* 9:1169–1172.
5. Mastrorade DN (2005) Automated electron microscope tomography using robust prediction of specimen movements. *J Struct Biol* 152:36–51.
6. Kremer JR, Mastrorade DN, McIntosh JR (1996) Computer visualization of three-dimensional image data using IMOD. *J Struct Biol* 116:71–76.

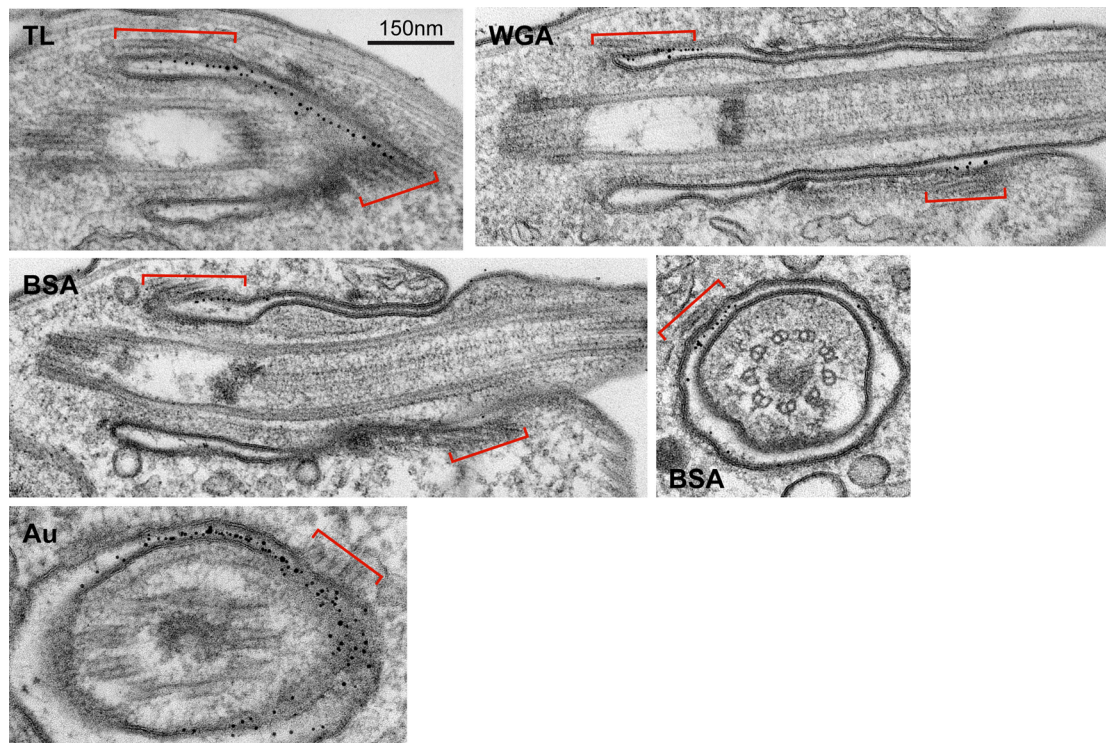


Fig. S1. Endocytic markers accumulate specifically at the membrane abutting the 4MT when endocytosis is blocked by cold treatment of bloodstream-form trypanosomes. Representative thin sections of the FP of cells incubated for 15 min on ice with 5-nm gold conjugated to TL, WGA, or BSA or unconjugated 5-nm gold (Au). Red bars indicate the positions at which the 4MT pass through the section.

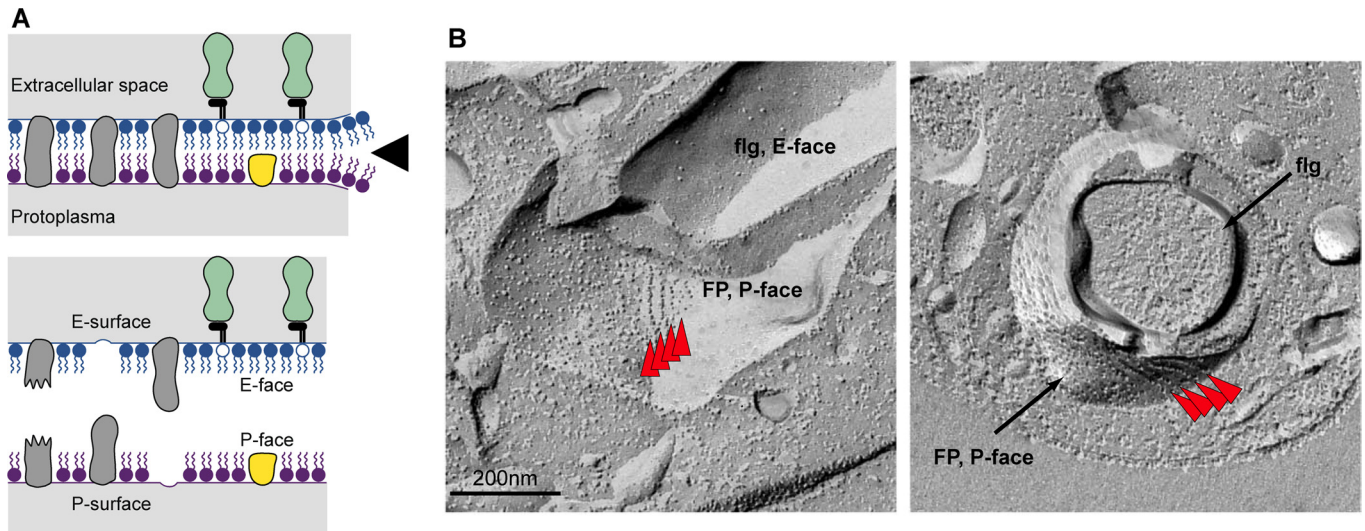


Fig. S2. The flagellar pocket membrane. **A** illustrates how the P-face and E-face views in **B** and Figs. 4 and 5 are produced by freeze fracture. As the membrane is split along its hydrophobic interior (black arrowhead), transmembrane proteins are partitioned with one or other of the half-membrane leaflets; they are then visualized as particles by platinum–carbon shadowing. GPI-anchored proteins are illustrated in light green, along with the GPI anchor (black) and transmembrane proteins (gray). **(B)** Linear arrangements of IMPs, suggestive of an association with the 4MT, are occasionally viewed on the P face of the FP membrane (red arrowheads). Platinum–carbon shadow direction is from bottom to top (*Left*) and from top to bottom (*Right*) to enable morphological matching between the images.

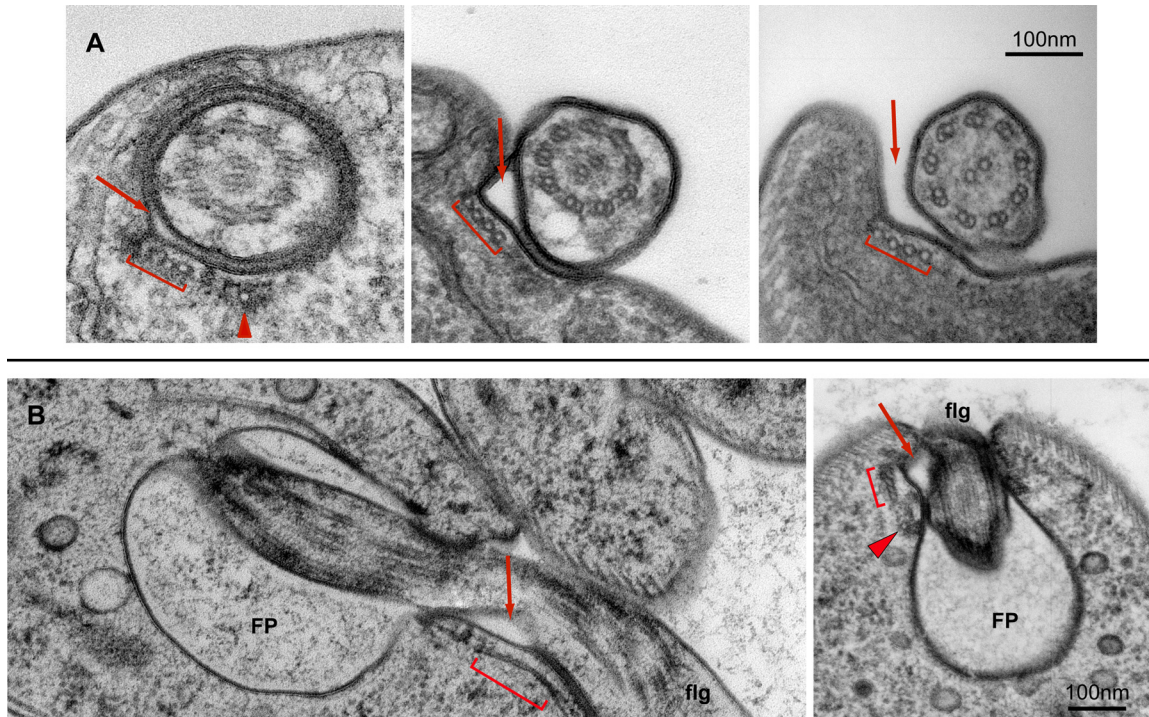


Fig. 53. The channel is consistently found in cells from different treatments and fixations. (A) Transverse thin-section electron micrographs of the neck and flagellum exit site in cells fixed in culture at 37 °C in the absence of gold particles, where the gap between the two membranes is seen (red arrow). (B) The channel (red arrow) along the neck region is also seen in cells cryoimmobilized by high-pressure freezing, followed by freeze-substitution fixation. Longitudinal (*Left*) and transverse (*Right*) thin sections of the FP and flagellum (flg) exit site. Red bar indicates the positions at which the 4MT pass through the section, and red arrowhead points to the neck microtubule.

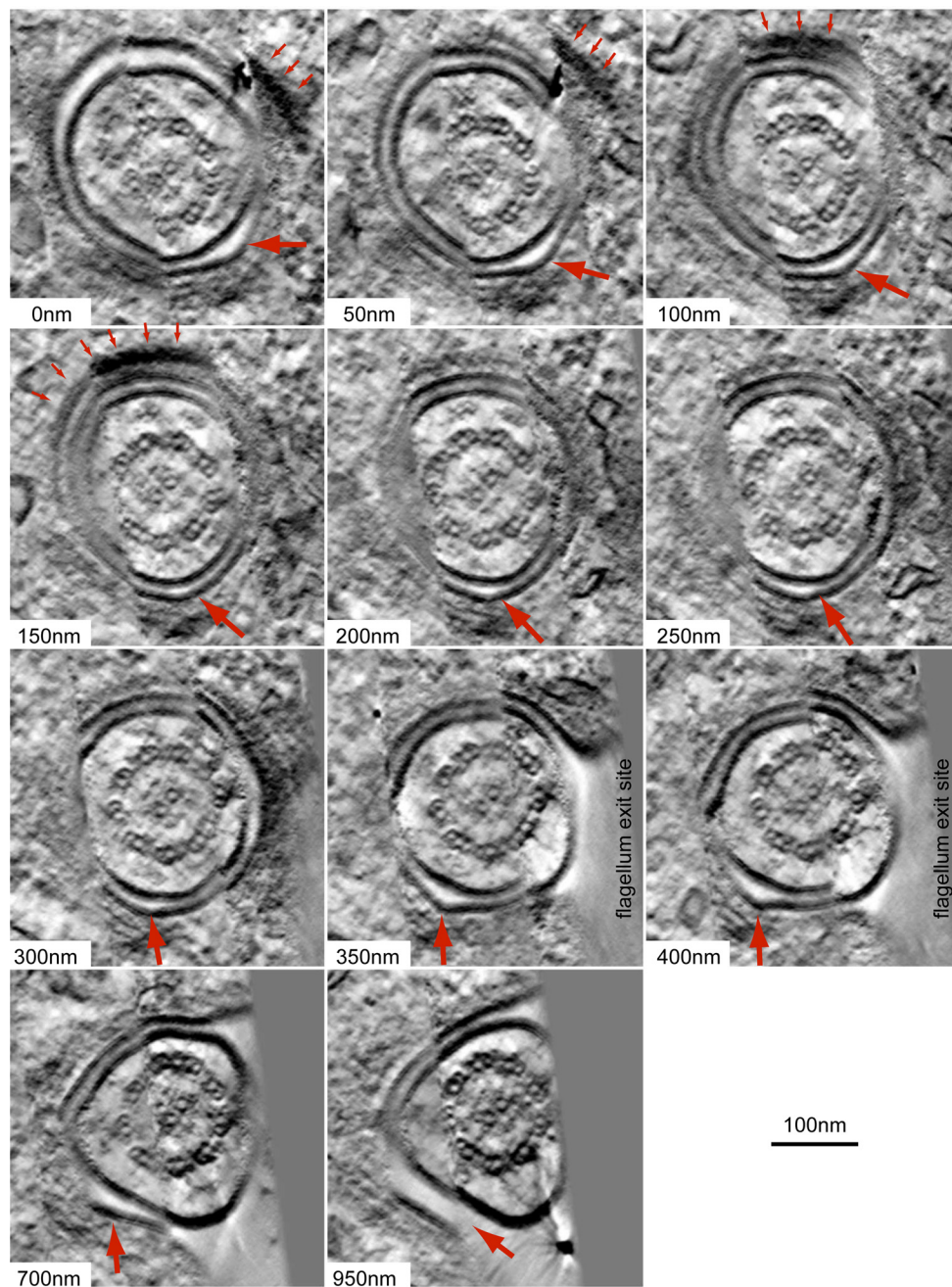
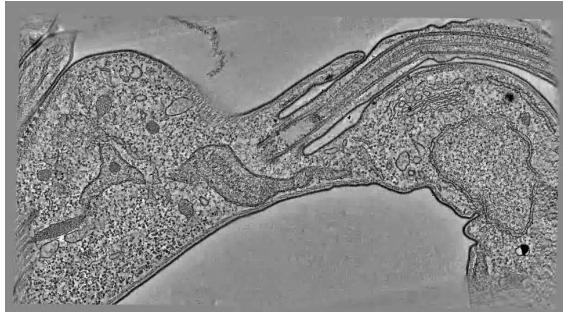
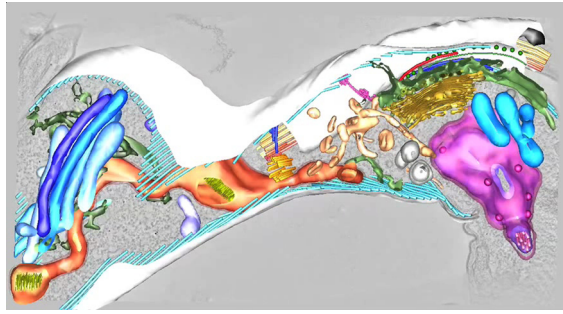


Fig. S4. The channel forms a continuous luminal space between the FP and the extracellular milieu. Tomographic slices through the length of the neck region, from the most superficial point of the pocket (*Top Left*), where the collar (small red arrows) constricts its circumference, to the point in which the flagellum exits the cell (*Bottom Right*). Large red arrow points to the channel. Length units in white boxes represent the distance between any two slices.



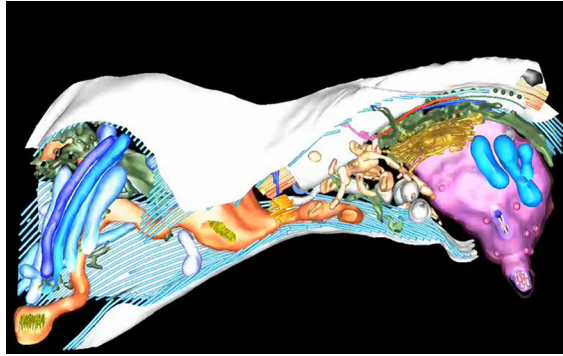
Movie S1. 3D electron tomographic reconstruction of the anterior FP region and surrounding organelles from a late-M-phase bloodstream-form trypanosome. This reconstruction is derived from a 3×1 montaged, three-serial section tomogram yielding a total of 457 tomographic slices.

[Movie S1 \(MOV\)](#)



Movie S2. 3D electron tomographic reconstruction seen in [Movie S1](#) merged with the resultant 3D segmentation model (which can be seen in [Movie S3](#)).

[Movie S2 \(MOV\)](#)



Movie S3. 3D segmentation model of the major organelles and ultrastructural features present in the electron tomographic reconstruction shown in [Movie S1](#). The plasma membrane and subpellicular microtubules along one side of the model have been left off the model to allow better visualization of the features inside the cell. For color code, please see the legend for Fig. 2.

[Movie S3 \(MOV\)](#)